

2

AD-A216 454



DEGENERATE FOUR WAVE MIXING FROM A WAVEGUIDE WITH GUIDED WAVE PUMP BEAMS

G.I. Stegeman
E.M. Wright
C.T. Seaton

Optical Sciences Center
University of Arizona
Tucson, AZ 85721

November 1989

Final Report

Approved for public release; distribution unlimited.

DTIC
ELECTE
DEC 21 1989
S B D

**Weapons Laboratory
Air Force Systems Command
Kirtland Air Force Base, NM 87117-6008**

This final report was prepared by the Optical Sciences Center, University of Arizona, Tucson, Arizona, under Contract F29601-87-C-0052, Job Order 2301Y401 with the Weapons Laboratory, Kirtland Air Force Base, New Mexico. Dr Christopher M. Clayton (AROM) was the Laboratory Project Officer-in-Charge.

When Government drawings, specifications, or other data are used for any purpose other than in connection with a definitely Government-related procurement, the United States Government incurs no responsibility or any obligation whatsoever. The fact that the Government may have formulated or in any way supplied the said drawings, specifications, or other data, is not to be regarded by implication, or otherwise in any manner construed, as licensing the holder, or any other person or corporation; or as conveying any rights or permission to manufacture, use, or sell any patented invention that may in any way be related thereto.

This report has been authored by a contractor of the United States Government. Accordingly, the United States Government retains a nonexclusive, royalty-free license to publish or reproduce the material contained herein, or allow others to do so, for the United States Government purposes.

This report has been reviewed by the Public Affairs Office and is releasable to the National Technical Information Service (NTIS). At NTIS, it will be available to the general public, including foreign nations.

If your address has changed, if you wish to be removed from our mailing list, or if your organization no longer employs the addressee, please notify WL/AROM, Kirtland AFB, NM 87117-6008 to help us maintain a current mailing list.

This technical report has been reviewed and is approved for publication.

Christopher M. Clayton

CHRISTOPHER M. CLAYTON, PhD
Project Officer

Lee P. Schelonka

LEE P. SCHELONKA
Captain, USAF
Chief, Quantum Optics Branch

FOR THE COMMANDER

Harro Ackermann

HARRO ACKERMANN
Lt Col, USAF
Chief, Optics Division

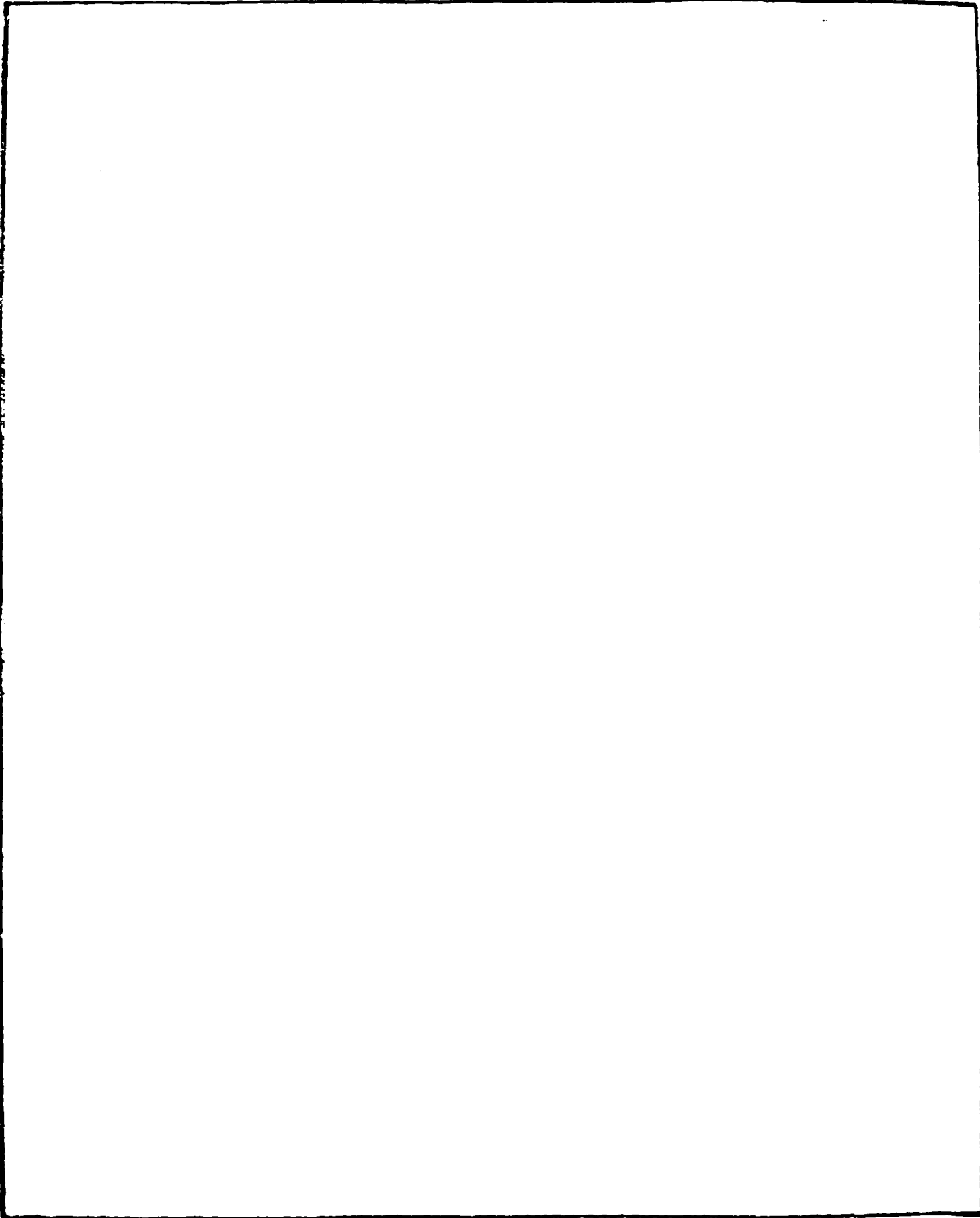
DO NOT RETURN COPIES OF THIS REPORT UNLESS CONTRACTUAL OBLIGATIONS OR NOTICE ON A SPECIFIC DOCUMENT REQUIRES THAT IT BE RETURNED.

REPORT DOCUMENTATION PAGE

1a. REPORT SECURITY CLASSIFICATION UNCLASSIFIED			1b. RESTRICTIVE MARKINGS	
2a. SECURITY CLASSIFICATION AUTHORITY			3 DISTRIBUTION/AVAILABILITY OF REPORT Approved for public release; distribution unlimited.	
2b. DECLASSIFICATION/DOWNGRADING SCHEDULE				
4. PERFORMING ORGANIZATION REPORT NUMBER(S)			5 MONITORING ORGANIZATION REPORT NUMBER(S) WL-TR-89-49	
6a. NAME OF PERFORMING ORGANIZATION Optical Sciences Center	6b. OFFICE SYMBOL (if applicable)	7a. NAME OF MONITORING ORGANIZATION Weapons Laboratory		
6c. ADDRESS (City, State, and ZIP Code) University of Arizona Tucson, Arizona 85721		7b. ADDRESS (City, State, and ZIP Code) Kirtland Air Force Base, NM 87117-6008		
8a. NAME OF FUNDING/SPONSORING ORGANIZATION	8b. OFFICE SYMBOL (if applicable)	9 PROCUREMENT INSTRUMENT IDENTIFICATION NUMBER F29601-87-C-0052		
8c. ADDRESS (City, State, and ZIP Code)		10 SOURCE OF FUNDING NUMBERS		
		PROGRAM ELEMENT NO 61102F	PROJECT NO. 23	TASK NO. 01
		WORK UNIT ACCESSION NO. Y401		
11 TITLE (Include Security Classification) DEGENERATE FOUR WAVE MIXING FROM A WAVEGUIDE WITH GUIDED WAVE PUMP BEAMS				
12. PERSONAL AUTHOR(S) Stegeman, G.I.; Wright, E.M.; and Seaton, C.T.				
13a. TYPE OF REPORT Final	13b. TIME COVERED FROM 15Jul87 to 15Jan88	14. DATE OF REPORT (Year, Month, Day) 1989 November	15 PAGE COUNT 24	
16. SUPPLEMENTARY NOTATION <i>See 4th from top, 1</i> <i>Keywords:</i>				
17. COSATI CODES			18. SUBJECT TERMS (Continue on reverse if necessary and identify by block number)	
FIELD	GROUP	SUB-GROUP	Nonlinear optics; Four wave mixing Solitons; Soliton transfer. (AW)	
19 ABSTRACT (Continue on reverse if necessary and identify by block number) We have analyzed the problem of degenerate four wave mixing in which a probe beam is incident from above onto a thin film waveguide pumped by two oppositely propagating guided waves. Four wave mixing signals are obtained both on reflection from the film surface, and on transmission into the substrate supporting the film. Analytical formulae are evaluated for a number of different cases which compare nonlinearities in the film versus the substrate. <i>Cont'd Pg. 2</i>				
20. DISTRIBUTION/AVAILABILITY OF ABSTRACT <input checked="" type="checkbox"/> UNCLASSIFIED/UNLIMITED <input type="checkbox"/> SAME AS RPT <input type="checkbox"/> DTIC USERS			21 ABSTRACT SECURITY CLASSIFICATION UNCLASSIFIED	
22a. NAME OF RESPONSIBLE INDIVIDUAL CHRISTOPHER M. CLAYTON, PhD			22b. TELEPHONE (Include Area Code) (505) 844-0475	22c. OFFICE SYMBOL AROM

UNCLASSIFIED

SECURITY CLASSIFICATION OF THIS PAGE



UNCLASSIFIED

SECURITY CLASSIFICATION OF THIS PAGE

1. Introduction

cont'd
Degenerate four-wave mixing has a number of potential applications for retro-reflectors, correction of phase aberrations, laser resonators, signal processing etc.¹ Most previous investigations of degenerate four wave mixing (DFWM) have considered bulk media and focussed gaussian beams. In such experiments it is impossible to maintain collimated beams over long distances due to diffraction, thus limiting the quality of the DFWM signal.

Guided wave geometries offer some potentially useful approaches to DFWM.²⁻⁴ The strong beam confinement results in high power densities and indeed efficient DFWM has been demonstrated in both fibers² and planar waveguides.³ In this paper we discuss the case in which the two pump beams are guided, and the probe beam is incident from outside the waveguide onto the film surface. For planar waveguides, DFWM has been discussed previously for the cases of all four waves guided,⁵ and for pump beams incident on a waveguide with a guided probe beam.⁶ To the best of our knowledge, the case of two guided pump beams and an externally incident probe beam has not been addressed before. It is an interesting geometry for three reasons. Firstly, the four-wave mixing of an incident plane wave occurs effectively over an interaction distance of a micron, decreasing the effects of distortion etc. Secondly, despite the short interaction distance, the efficiencies can still be high due to the high power densities available with guided waves, i.e. very high pump beam powers are not necessary. Thirdly, a DFWM signal is obtained on transmission and is separated in angle from the incident probe beam. This means that the DFWM signal can be accessed without using a beamsplitter to separate the probe and conjugate signals.

This paper is organized as follows. In the next section, we summarize briefly the formal aspects of the calculation: the details are left to the Appendix. Section 3 is devoted to the presentation of numerical results, and a discussion of their significance. The paper is summarized in Section 4.

Keyed to Pg 1

Distribution/	
Availability Codes	
Dist	Avail and/or Special
A-1	

2. Analysis of the Problem

The DFWM geometry analysed here is shown in Fig 1. The counter-propagating pump beams are both assumed to be TE_m guided waves, that is the electric field polarization is the y-direction. (We do not treat the TM case here, although we do not expect anything substantially different except for the existence of a Brewster angle phenomenon.) The probe signal is incident from above the thin film waveguide in the form of a plane wave at an angle θ_c relative to the normal. In addition to the usual reflected DFWM signal, there is also a "transmitted" DFWM signal whose origin will be discussed in some detail later.

We now outline the formal analysis. To facilitate the understanding of the DFWM process, we write the TE fields of frequency ω guided by a film of thickness "h" in the cladding, film and substrate (subscripted c, f and s respectively) as

$$E_z(r,t) = \frac{1}{2} e_y E_z(r,\omega) e^{-i\omega t} + \text{c.c.} = \frac{1}{2} C_{TE} P_z^{1/2} e_y f(x) e^{i(\pm \beta k_0 z - \omega t)} + \text{c.c.} \quad (1)$$

$$f(x) = e^{q_c k_0 x}, \quad q_c^2 = \beta^2 - n_c^2 : x < 0, \quad (2a)$$

$$f(x) = A_{f+} e^{i k_0 q_f x} + A_{f-} e^{-i k_0 q_f x}, \quad q_f^2 = n_f^2 - \beta^2 : h > x > 0,$$

$$A_{f+} = \frac{1}{2} \left[1 - i \frac{q_c}{q_f} \right] = A_{f-}^*, \quad (2b)$$

$$f(x) = A_s e^{-q_s k_0 (x - h)}, \quad q_s^2 = \beta^2 - n_s^2 : x > h,$$

$$A_s = \cos(q_f k_0 h) + \frac{q_c}{q_f} \sin(q_f k_0 h). \quad (2c)$$

where the normalization constant

$$C_{TE} = \frac{2q_f}{\sqrt{\frac{\beta}{c\mu_0} h_{eff}(q_f^2 + q_c^2)}} \quad (3a)$$

$$h_{eff} = h + \frac{1}{q_c k_0} + \frac{1}{q_s k_0} \quad (3b)$$

allows P to be the guided wave power in watts per meter in the y -dimension. The effective index β is given by the usual dispersion relation

$$\tan(q_f k_0 h) = \frac{q_f(q_c + q_s)}{q_f^2 - q_f q_s} \quad (4)$$

We assume an external plane wave incident from the cladding medium. This incident beam undergoes multiple reflections inside the film and is partially reflected into the cladding (air), and partially transmitted into the substrate. We write this field as

$$E_{inc}(r,t) = \frac{1}{2} e_y E_{inc}(r,\omega) e^{-i\omega t} + c.c. = \frac{1}{2} e_y g(x) e^{i(\kappa_p k_0 z - \omega t)} + c.c., \quad (5)$$

$$\kappa_p = n_c \sin \theta_c$$

$$g(x) = e^{i\kappa_c k_0 x} + B_r e^{-i\kappa_c k_0 x}, \quad \kappa_c = n_c \cos \theta_c : x < 0, \quad (6a)$$

$$g(x) = B_{r+} e^{i\kappa_f k_0 x} + B_{r-} e^{-i\kappa_f k_0 x}, \quad \kappa_f^2 = n_f^2 - \kappa_p^2 : h > x > 0, \quad (6b)$$

$$g(x) = B_s e^{i\kappa_s k_0 (x - h)}, \quad \kappa_s^2 = n_s^2 - \kappa_p^2 : x > h. \quad (6c)$$

Solving the boundary condition problem in the usual way gives

$$B_{T-} = \frac{2\kappa_c(\kappa_f - \kappa_s)}{(\kappa_f + \kappa_s)(\kappa_f + \kappa_c)\exp[-2iW] + (\kappa_c - \kappa_f)(\kappa_f - \kappa_s)} \quad (7a)$$

$$B_{T+} = \frac{2\kappa_c(\kappa_f + \kappa_s)\exp[-2iW]}{(\kappa_f + \kappa_s)(\kappa_f + \kappa_c)\exp[-2iW] + (\kappa_c - \kappa_f)(\kappa_f - \kappa_s)} \quad (7b)$$

$$B_s = B_{T+} e^{iW} + B_{T-} e^{-iW} \quad (7c)$$

where $W = \kappa_f k_0 h$.

The calculation of the nonlinear polarization associated with the DFWM signal is relatively straightforward.^{1,5} Including the degeneracy factor,

$$P_y^{NL}(r) = 4\epsilon_0 n_{2E}(x) E_+(\omega) E_-(\omega) E_{inc}^*(\omega) \quad (8)$$

where n_{2E} is defined in the usual way as a field-dependent refractive index of the form $n(I) = n_0 + n_{2E}I$ (and I is the local intensity). To isolate the different contributions to the DFWM signal, we write

$$P_y^{NL}(r) = \sum_p P_y^{NL}(p) e^{i(-\kappa_p k_0 z + p k_0 x)} \quad (9)$$

For the film region,

$$P_y^{NL}(2q_f - \kappa_f) = 4\epsilon_0 n_f n_{2Ef} C_{TE}^2 A_{f+}^2 B_{f+}^* \quad (10a)$$

$$P_y^{NL}(2q_f + \kappa_f) = 4\epsilon_0 n_f n_{2Ef} C_{TE}^2 A_{f+}^2 B_{f-}^* . \quad (10b)$$

$$P_y^{NL}(-\kappa_f) = 8\epsilon_0 n_f n_{2Ef} C_{TE}^2 A_{f+} A_{f-} B_{f+}^* . \quad (10c)$$

$$P_y^{NL}(+\kappa_f) = 8\epsilon_0 n_f n_{2Ef} C_{TE}^2 A_{f+} A_{f-} B_{f-}^* . \quad (10d)$$

$$P_y^{NL}(-2q_f - \kappa_f) = 4\epsilon_0 n_f n_{2Ef} C_{TE}^2 A_{f-}^2 B_{f+}^* . \quad (10e)$$

$$P_y^{NL}(-2q_f + \kappa_f) = 4\epsilon_0 n_f n_{2Ef} C_{TE}^2 A_{f-}^2 B_{f-}^* . \quad (10f)$$

The dominant wavevector matched terms occur at $p = -\kappa_f$ for DFWM signal travelling upwards in the film, and at $p = \kappa_f$ for the signal generated in the downwards direction in the film. Multi-reflections occurring in the film result in DFWM both on reflection and transmission through the film. Although none of the other terms are wavevector matched, they also contribute to the DFWM signals because the guiding films are typically a wavelength thick.

A DFWM polarization also can occur inside the substrate. Here

$$P_y^{NL}(-\kappa_s + 2iq_s) = 4\epsilon_0 n_s n_{2Es}(x) A_s^2 C_{TE}^2 B_s^* e^{ipk_0 h} . \quad (11)$$

which generates a wavevector matched DFWM signal travelling upwards towards the film-substrate interface.

The strength of the DFWM signal on reflection and transmission is calculated by solving the polarization driven wave equation for fields with wavevector component $-\kappa_p k_0$ parallel to the surface, i.e.

$$\left[-\kappa_r^2 - \frac{1}{k_0^2} \frac{d^2}{dx^2} \right] E_y(\omega, x) = \sum_p \frac{1}{\epsilon_0} P_y^{NL}(p) e^{ipk_0 x}, \quad (12a)$$

where

$$E_s(r, t) = \frac{1}{2} e_y E_y(\omega, x) e^{i(-\kappa_p k_0 z - \omega t)} + c.c. \quad (12b)$$

The form of the DFWM signal fields far from the film is given by

$$E_y(\omega, x) = D_c e^{-i\kappa_c k_0 x} \quad x < 0, \quad (13a)$$

$$E_y(\omega, x) = D_s e^{i\kappa_s k_0 (x-h)} \quad x > h. \quad (13b)$$

From Eqn. (6a), and noting that the intensity S is given by $1/2 n_0 c \epsilon_0 |E_y|^2$, the (intensity) DFWM reflection and transmission coefficients are given by

$$R = \frac{S_r}{S_{inc}} = |D_c|^2 = \eta_r P_+ P_- \quad (14a)$$

$$T = \frac{S_t}{S_{inc}} = \frac{n_s}{n_c} |D_s|^2 = \eta_t P_+ P_- \quad (14b)$$

A variety of techniques can be used to solve Eqns. (12) for R and T . We outline in the Appendix a technique in which the total fields generated by the nonlinear polarization source terms are evaluated. The interested reader can find the details there. Here we shall proceed to the numerical evaluation of R and T .

3. Numerical Results

Numerical calculations were performed on two representative guided wave film geometries, both utilizing typical nonlinear organic parameters. In the first case, the following parameters were assumed:⁷ $n_c = 1$, $n_f = 1.6$, $n_s = 1.45$, $\lambda = 1.06 \mu\text{m}$, $n_{2F} = 10^{-16} \text{ m}^2/\text{W}$ and $n_{2S} = 0$. In the second case, the effect of a nonlinearity in the substrate instead of the film was examined with $n_{2F} = 0$, and $n_{2S} = 10^{-16} \text{ m}^2/\text{W}$. Relatively large oscillations in the DFWM cross-section were observed for both cases, and two additional calculations were performed with a smaller difference between the film and substrate refractive indices, namely $n_f = 1.6$ and $n_s = 1.59$.

Figs. 2 and 3 show η_r and η_t , respectively, as a function of incidence angle θ_c . For film thickness near waveguide cut-off, the externally incident beam does not show any resonances across the film and the variation in the cross-sections η_r and η_t is smooth with angle. However, as the film thickness is increased and resonances begin to appear across the film, distinct maxima and minima in the cross-section appear, their number increasing with film thickness. Since the transmitted DFWM signal requires reflection at the lower film boundary, the oscillations are much larger on transmission than on reflection. Therefore it appears feasible to optimize the signal for a given film thickness by varying the incidence angle.

The origin of the transmitted DFWM signal is fairly obvious. Because reflections occur at both film boundaries, the incident wave forms a standing wave in the film. Hence the DFWM signal travelling upwards in the film and reflected at the film-cladding boundary, and the DFWM signal from the incident wave travelling upwards in the film due to reflection at the film-substrate boundary both contribute to DFWM on transmission. However, because the reflection coefficients at the film interfaces are small, the DFWM signal on transmission is much smaller than that on reflection. On the other hand, it is "background-free" in the sense that there is no other beam in this direction in space, in contrast to the case on reflection where stray scattering from a

beamsplitter limits the signal to noise ratio.

The variation in η with film thickness at a 45° incident angle is shown in Fig. 4. As expected, oscillations again occur due to multireflections of both the incident and signal beams in the film. When the index difference between the film and substrate is reduced, the amplitude of the oscillations is also reduced, as shown in Fig. 5.

The effectiveness of using a linear film on a nonlinear substrate is examined in Fig. 6. Clearly the cross-section decreases rapidly from its cut-off value and falls orders of magnitude below that obtained on reflection.

We now compare the detailed behaviour shown in the preceding figures with an approximation based on plane wave analysis. It is well known that for plane waves in the small signal limit⁸

$$R = \frac{S_r}{S_{inc}} = \left[\frac{4\pi L n_{21}}{\lambda} \right]^2 S_+ S_- \quad (15)$$

where $n = n_0 + n_{21}S$, L is the interaction distance. To a useful approximation $S_+ = P_+/h_{eff}$ where h_{eff} is the effective waveguide thickness, as defined in Eqn. (3b). Therefore, rewriting for the guided wave case,

$$R = \left[\frac{4\pi L n_{21}}{h_{eff} \lambda} \right]^2 P_+ P_- \quad (16)$$

should provide a useful approximation. For thick films, $h_{eff} \approx h \approx L$ and the cross-section coefficient becomes independent of film thickness. Estimating for the present case, we obtained 0.16×10^{-17} for the cross-section, in good agreement with the "average" value of the oscillations of 0.2×10^{-17} shown in Figs. 4 and 5. Despite the fact that

$h = L$ is usually good to at best $\pm 25\%$. Eqn. (16) does give a useful value for the cross-section. In addition it predicts the asymptotic behavior with increasing film thickness. Furthermore, since $h_{\text{eff}} \rightarrow \infty$ at cut-off where the substrate field degenerates into a plane wave travelling parallel to the surface, $R \rightarrow 0$ at cut-off can also be understood. Finally, it is clear that the asymptotic value of the cross-section with film thickness depends primarily on the nonlinearity of the film, and not the details of the waveguiding structure.

Equations 15 and 16 also provide some insight into the maximum values of reflectivity that might be available. Assuming power densities approaching damage values, for example 10 GW/cm^2 , and $1 \text{ }\mu\text{m}$ thick films, this corresponds to $P \approx 10^7 \text{ W/m}$ leading to a maximum reflectivity of 0.02 (2%). (For 1 cm guided wave beam, a peak power of only 100 KW is required for the pump beams.) Hence, for this material system, pump wave depletion can be ignored. For semiconductor materials (which also exhibit large absorption), reflectivities in excess of 100% should be possible.

This work was supported by the Air Force Weapons Laboratory (F29601-87-C-0052), and the Air Force Office of Scientific Research (AFOSR-87-0344).

Appendix

In this appendix we discuss the details of the solution of the polarization driven wave equation (12a). The nonlinear polarization source terms are given by Eqns. 8-11. The solution fields can be separated, for convenience, into the solutions of the inhomogeneous wave equation ($P_y \neq 0$) and the homogeneous wave equation ($P_y = 0$). The solutions to the driven wave equation do not by themselves satisfy the usual electromagnetic boundary conditions. Hence it is necessary to also include solutions to the sourceless wave equation. For the cladding and substrate regions these are given by Eqns. (13), and for the film by

$$E_y(\omega, x) = D_{r+} e^{i\kappa_r k_0 x} + D_{r-} e^{-i\kappa_r k_0 x}, \quad x > h > 0. \quad (A-1)$$

The structure of the polarization driven fields is determined by the form of the polarization source terms given in Eqns. (9-11). For the film region, we write

$$E_y(r, t) = \sum_p \frac{1}{2} E_y(p, x) e^{i(-\kappa_p k_0 z - \omega t)} + \text{c.c.} \quad (A-2)$$

Solving gives

$$E_y(p, x) = \frac{P_y(p)}{p^2 - \kappa_r^2} e^{ipk_0 x}. \quad (A-3)$$

Clearly there is a divergence for the case $p = \pm \kappa_r$ which must be treated separately. Recalling that we are free to add or subtract solutions to the homogeneous wave equation, we write for $p = \pm \kappa_r$

$$E_y(p, x) = \frac{P_y(p)}{p^2 - \kappa_r^2} e^{ipk_0 x} [1 - e^{i(\pm \kappa_r - p)k_0 x}]. \quad (A-4)$$

Expanding the exponential within the square brackets for small arguments gives

$$E_y(\pm \kappa_r, x) = \pm i \frac{k_0 x}{2\kappa_r} P_y(\pm \kappa_r) e^{\pm i\kappa_r k_0 x}. \quad (A-5)$$

thus eliminating the mathematical divergence. Furthermore, for the substrate region $p = -\kappa_s + i2q_s$ and

$$E_y(p, x) = \frac{P_y(p)}{p^2 - \kappa_s^2} e^{ik_0 p(x-h)} \quad (\text{A-6})$$

Similarly, the $H_z(p, x)$ can be calculated from Maxwell's equations.

Equations A-3 to A-6 describe the polarization driven fields, i.e. solutions to the inhomogeneous wave equation. They can be evaluated at the film surfaces, for example on the film side, to give

$$E_y(0) = \sum_{p^2 \neq \kappa_f^2} \frac{P_y(p)}{p^2 - \kappa_f^2} \quad (\text{A-7})$$

$$\begin{aligned} E_y(h) = \sum_{p^2 \neq \kappa_f^2} \frac{P_y(p) e^{ipk_0 h}}{p^2 - \kappa_f^2} + i \frac{k_0 h}{2\kappa_f} \left[P_y(\kappa_f) e^{i\kappa_f k_0 h} - P_y(-\kappa_f) e^{-i\kappa_f k_0 h} \right] \\ + \frac{P_y(-\kappa_s + 2iq_s)}{4i\kappa_s q_s + 4q_s^2} \end{aligned} \quad (\text{A-8})$$

$$c\mu_0 H_z(0) = \sum_{p^2 \neq \kappa_f^2} \frac{pP_y(p)}{p^2 - \kappa_f^2} + \frac{1}{2\kappa_f} [P_y(\kappa_f) - P_y(-\kappa_f)] \quad (\text{A-9})$$

$$c\mu_0 H_z(h) = \sum_{p^2 \neq \kappa_f^2} \frac{pP_y(p)}{p^2 - \kappa_f^2} e^{ipk_0 h}$$

$$\begin{aligned}
& + \frac{1}{2\kappa_f} \left[P_y(\kappa_f) e^{i\kappa_f k_0 h} (1 + i\kappa_f k_0 h) + P_y(-\kappa_f) e^{-i\kappa_f k_0 h} (-1 + i\kappa_f k_0 h) \right] \\
& + \frac{(-\kappa_s + 2iq_s) P_y(-\kappa_s)}{4iq_s \kappa_s + 4q_s^2} .
\end{aligned} \tag{A-10}$$

Clearly these fields do not constitute the complete solution since the usual tangential E_y and H_z fields are not continuous across the film boundaries. Therefore, it is necessary to include the solutions to the homogeneous wave equation, namely Eqns. (12b), (13), and (A-1) with the amplitudes D_c , D_{f+} , D_{f-} and D_s are adjusted to ensure continuity of the boundary conditions. Solving gives

$$D_c = \frac{D_{cn}}{D_d} . \tag{A-11}$$

$$\begin{aligned}
D_{cn} = & \kappa_f(\kappa_s \cos W - i\kappa_f \sin W) E_y(0) - \kappa_f \kappa_s E_y(h) + \kappa_f c \mu_0 H_z(h) \\
& - (\kappa_f \cos W + i\kappa_s \sin W) c \mu_0 H_z(0) .
\end{aligned} \tag{A-12}$$

$$D_d = \kappa_f(\kappa_s + \kappa_c) \cos W - i(\kappa_f^2 + \kappa_c \kappa_s) \sin W . \tag{A-13}$$

and

$$D_s = \frac{D_{sn}}{D_d} . \tag{A-14}$$

$$\begin{aligned}
D_{sn} = & -\kappa_f \kappa_c E_y(0) + \kappa_f(\kappa_c \cos W - i\kappa_f \sin W) E_y(h) - c \mu_0 \kappa_f H_z(0) \\
& + c \mu_0(\kappa_f \cos W - i\kappa_c \sin W) H_z(h) .
\end{aligned} \tag{A-15}$$

These results are then used in Eqns. (14) to evaluate the DFWM signals.

References

1. See for example, R. A. Fisher, ed., *Optical Phase Conjugation*, (Academic Press, New York, 1982).
2. S. M. Jensen and R. W. Hellwarth, *Appl. Phys. Lett.* 33, 404, (1978).
3. A. Gabel, K. W. DeLong, C. T. Seaton and G. I. Stegeman, *Appl. Phys. Lett.* 51, 1682 (1987).
4. G. I. Stegeman, C. T. Seaton and C. Karaguleff, *IEEE J. Quant. Electron.* QE-22, 1344 (1986).
5. C. Karaguleff and G. I. Stegeman, *IEEE J. Quant. Electron.* QE-20, 716 (1984).
6. E. Weinert-Raczka, *Opt. Commun.* 49, 2457 (1984).
7. G. M. Carter, J. V. Hryniewicz, M. K. Thakur, Y. J. Chen and S. E. Meyler, *Appl. Phys. Lett.* 49, 998 (1986).
8. A. Yariv, and D. M. Pepper, *Opt. Lett.* 1, 16 (1977).

Figure Captions

Fig. 1 The DFWM geometry analysed here. The pump beams are guided by a film of thickness h . A plane wave beam is incident from the cladding side and DFWM is obtained both on reflection and transmission through the film.

Fig. 2 The reflection DFWM cross-section η_r versus angle of incidence θ_c for three different film thicknesses. Here $n_c=1$, $n_f=1.6$, $n_s=1.45$, $n_{2If}=1 \times 10^{-16} \text{ m}^2/\text{W}$ and $n_{2Is}=0$.

Fig. 3 The transmission DFWM cross-section η_t versus angle of incidence θ_c for three different film thicknesses. Here $n_c=1$, $n_f=1.6$, $n_s=1.45$, $n_{2If}=1 \times 10^{-16} \text{ m}^2/\text{W}$ and $n_{2Is}=0$.

Fig. 4 The reflection (η_r) and transmission (η_t) DFWM cross-sections versus film thickness for $\theta_c=45^\circ$. Here $n_c=1$, $n_f=1.6$, $n_s=1.45$, $n_{2If}=1 \times 10^{-16} \text{ m}^2/\text{W}$ and $n_{2Is}=0$.

Fig. 5 The reflection (η_r) DFWM cross-section versus film thickness for $\theta_c=45^\circ$. Here $n_c=1$, $n_f=1.6$, $n_s=1.59$, $n_{2If}=1 \times 10^{-16} \text{ m}^2/\text{W}$ and $n_{2Is}=0$.

Fig. 6 The reflection ($\eta_r \equiv R$) and transmission ($\eta_t \equiv T$) DFWM cross-sections versus film thickness for $\theta_c=45^\circ$. For the solid line $n_c=1$, $n_f=1.6$, $n_s=1.45$, $n_{2Is}=1 \times 10^{-16} \text{ m}^2/\text{W}$ and $n_{2If}=0$. For the dotted line $n_c=1$, $n_f=1.6$, $n_s=1.59$, $n_{2Is}=1 \times 10^{-16} \text{ m}^2/\text{W}$ and $n_{2If}=0$.

Fig. 1

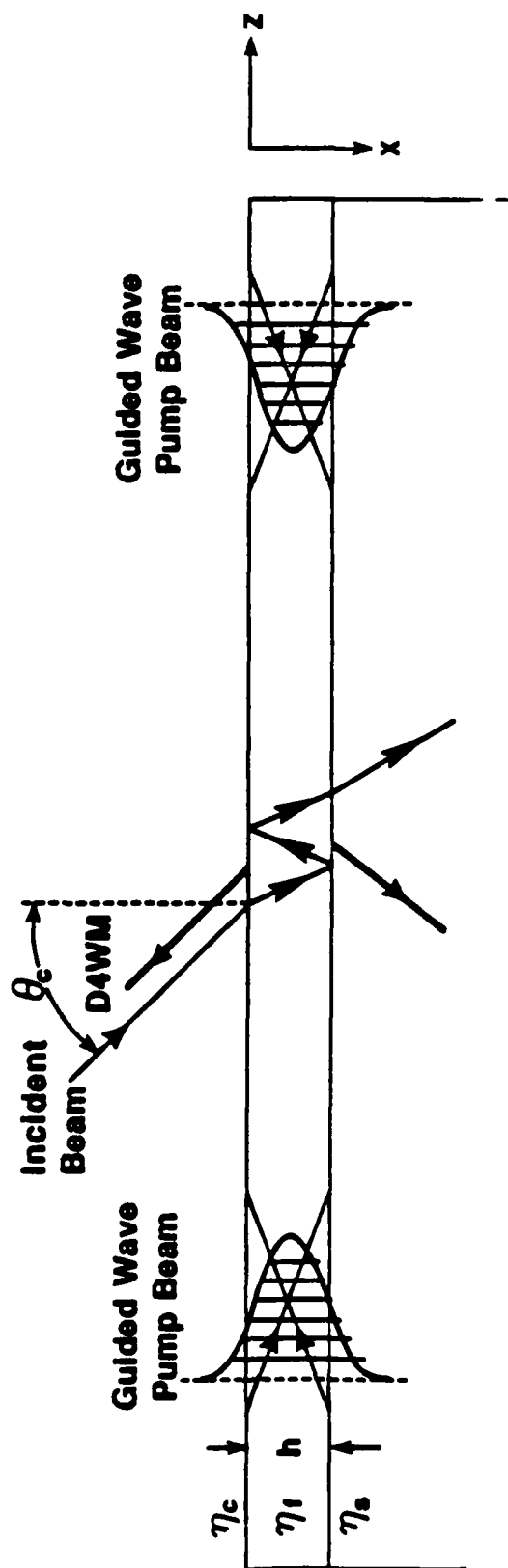


Fig. 2

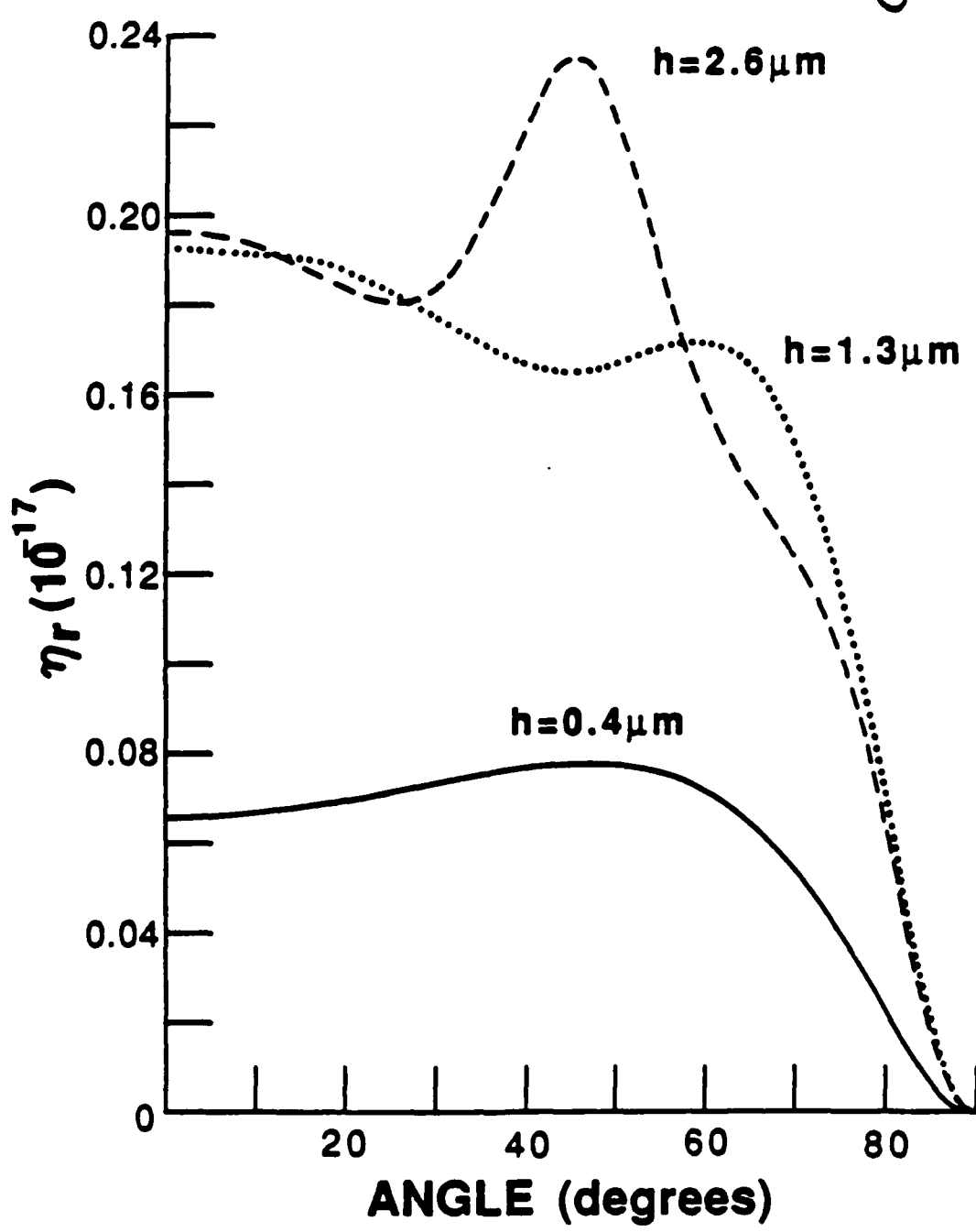


Fig. 3

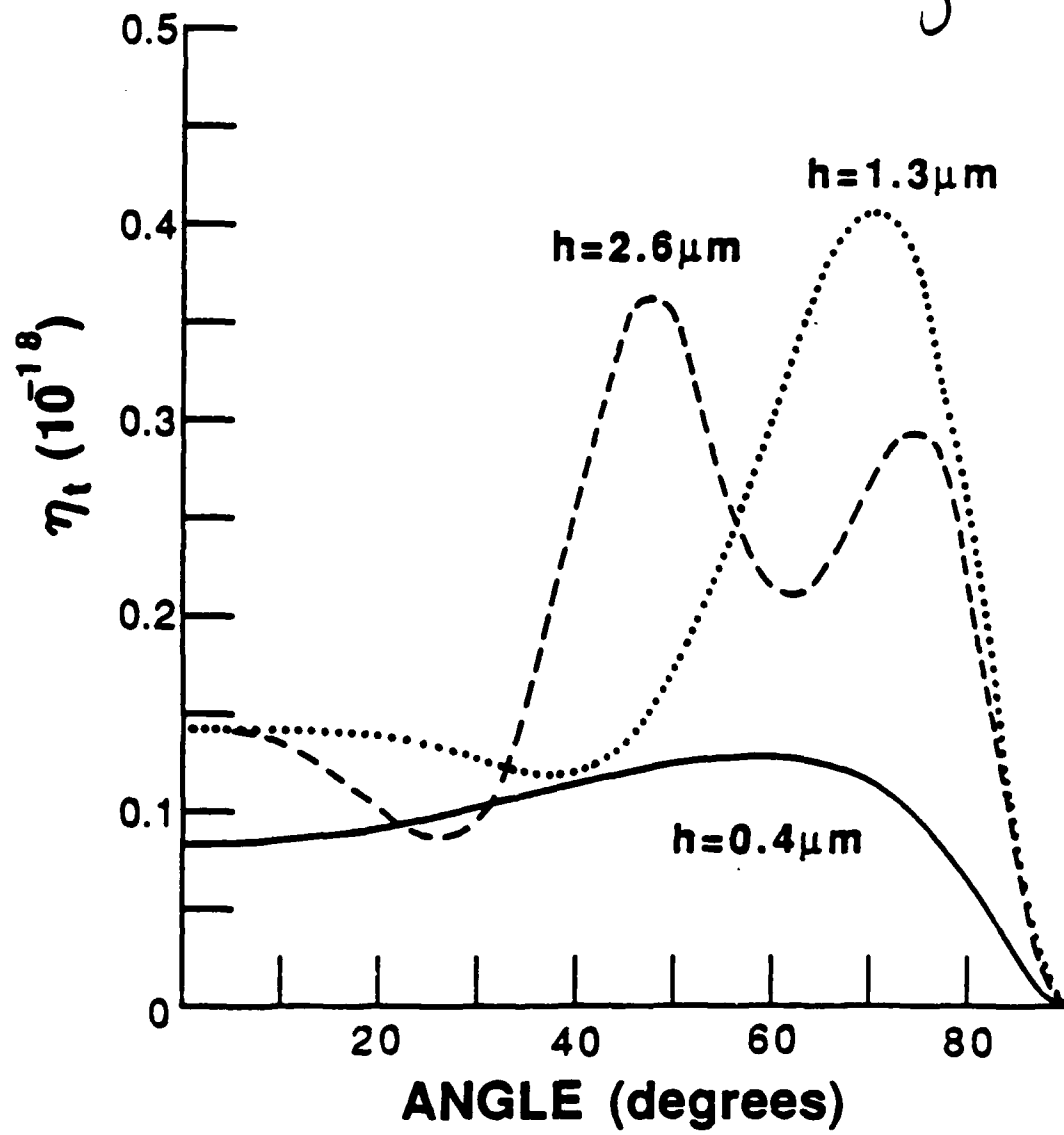


Fig. 4

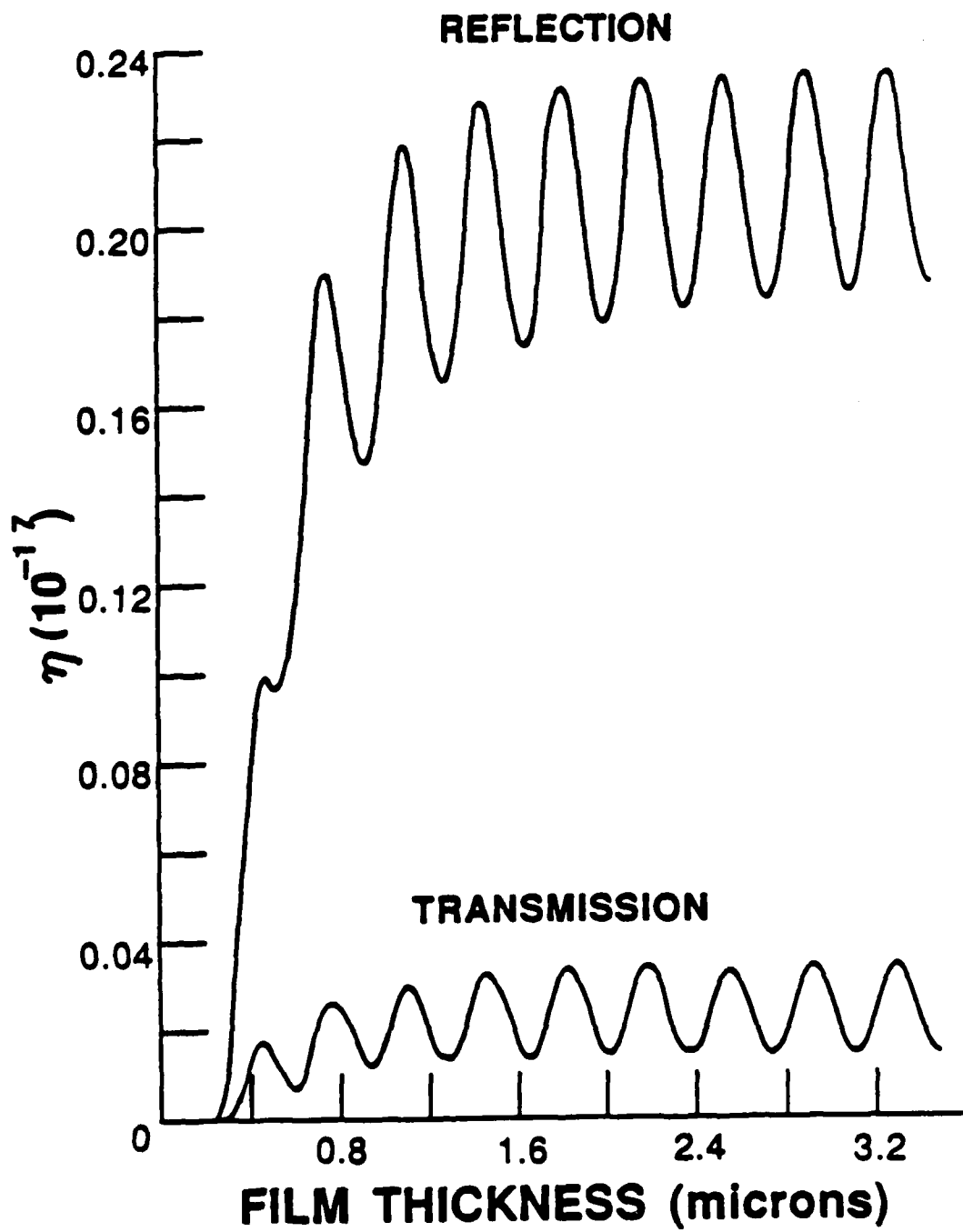


Fig: 5

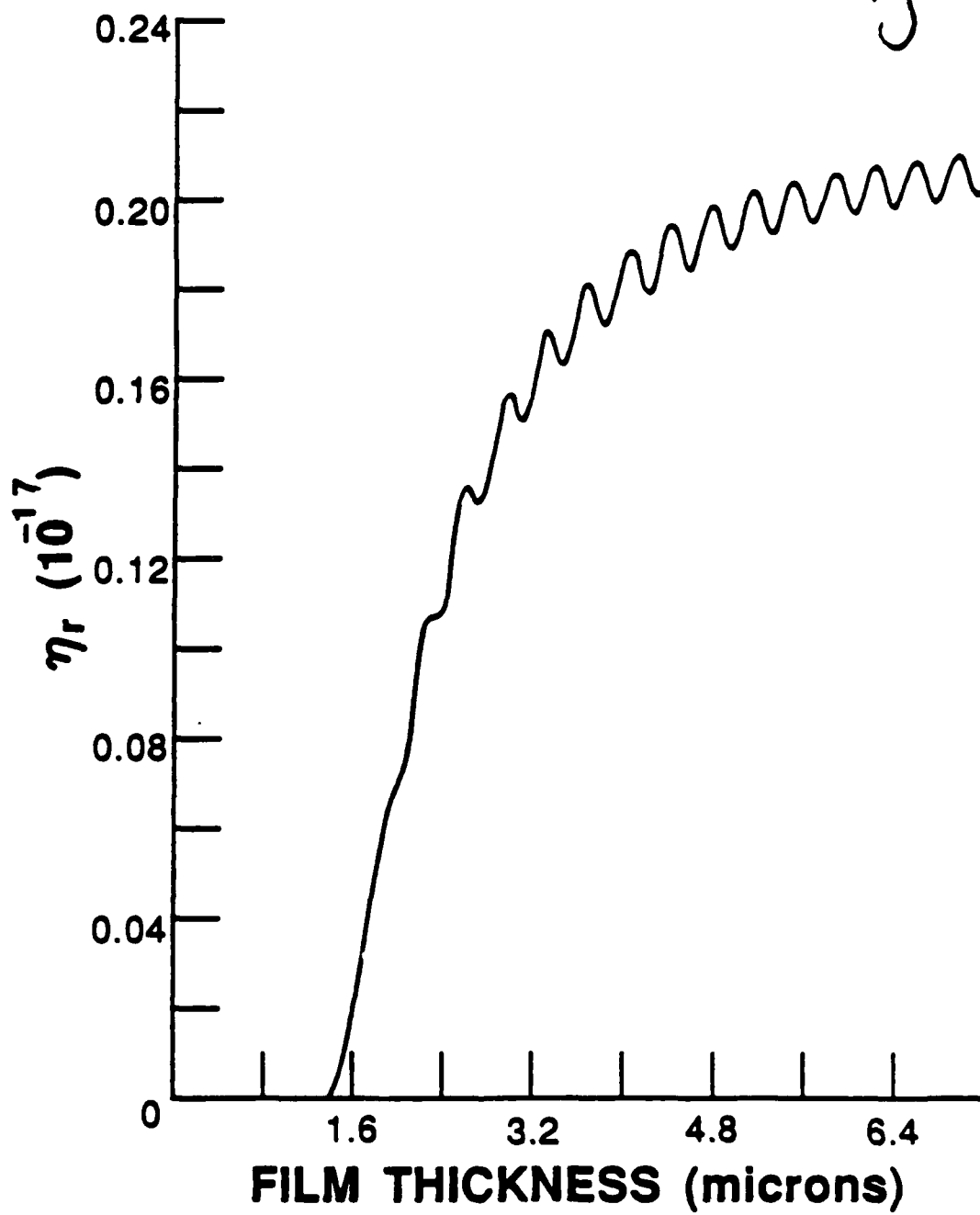


Fig. 6

